IEEE Access
Multidisciplinary | Rapid Review | Open Access Journal

Date of publication xxxx 00, 0000, date of current version xxxx 00, 0000.

Digital Object Identifier 10.1109/ACCESS.2017.Doi Number

A Head/Taillight Featuring Hybrid Planar Visible Light Communications/Millimetre Wave Antenna for Vehicular Communications

Mojtaba Mansour Abadi[1], Pavel Hazdra[2], Jan Bohata[2], Petr Chvojka[2], Paul Anthony Haigh[3], Zabih Ghassemlooy[1], and Stanislav Zvanovec[2]

[1]Optical Communications Research Group, Department of Mathematics, Physics and Electrical Engineering, Northumbria University, Newcastle upon Tyne, NE1 8ST, U.K

[2]Department of Electromagnetic Field, Faculty of Electrical Engineering, Czech Technical University in Prague, Technicka 2, 16627, Prague, Czech Republic

[3]Intelligent sensing and communications group, school of engineering, Newcastle University, NE1 7RU

Corresponding author: Mojtaba Mansour Abadi (e-mail: mojtaba.mansour@northumbria.ac.uk).

ABSTRACT With the emergence of the fifth generation and beyond mobile networks, both visible light communications (VLC) and radio frequency (RF) or millimetre wave (mmW) systems are expected to maintain the connectivity in various environments. In outdoor environments the link (VLC or RF) availability is paramount, which is affected by channel conditions. In particular, in vehicular communications other vehicles, harsh environment, and road geometry and structure will have the impact on the link connectivity and availability. In such cases, a front-end antenna solution, which benefits both optical and RF communication links, can be seen as an attractive option that can be fitted in future vehicles. In this paper, we present the design and practical implementation of a planar hybrid VLC/mmW antenna operating at 20.8 GHz and show measured results for characterization of RF and VLC links as well as communications performance. We have used the widely adopted on-off keying and quadrature amplitude modulation schemes with different orders to demonstrate data rates of 5 Mb/s and up to 100 Mb/s for the VLC and mmW links, respectively. By measuring the bit error rate and the error vector magnitude for VLC and Rf links, respectively for each modulation we have shown that the proposed hybrid planar antenna is suitable for example in a typical vehicle -to-vehicle communications.

INDEX TERMS VLC, mmW, Hybrid VLC/mmW, Hybrid VLC/RF, Hybrid Antenna

I. INTRODUCTION

Hybrid optical-radio frequency wireless technologies are an attractive solution for reliable outdoor communication links. They ensure reliability in all weather conditions whilst simultaneously relieving the pressure on radio frequency (RF) spectral usage at low cost and low complexity [1, 2]. As a result, optical/RF hybrid systems have become the focus of ever-increasing attention in recent years. A number of experimental demonstrations have shown improved reliability and reduced system outage [3], higher throughput [4] and lower power consumption [3]. Improved technological integration has also been demonstrated through advances in both soft [5], hard [6] and neural [7, 8] based switching modes between each transmission media [9].

Hybrid systems can broadly be classified as optical or RF, both of which have undergone substantial developments over the previous decades. For optical links, either infrared or visible light bands may be used to offer free space optics (FSO) and visible light communications (VLC), respectively. The advantages of FSO include high bandwidths and low power consumption [10], however, it is subject to eye safety conditions, which impose an upper limit on the optical transmit power. Therefore, VLC has become an attractive option in hybrid systems as it offers high power and bandwidth but with relaxed eye safety requirements. This comes at the cost of a less focused beam, which restricts the transmission distances. Note, using a laser with white light, the transmission distance can be increased further. On the other hand, the RF component has a high degree of customisability such as the

This article has been accepted for publication in a future issue of this journal, but has not been fully edited. Content may change prior to final publication. Citation information: DOI 10.1109/ACCESS.2020.3006992, IEEE Access

power, directionality, beamform and carrier frequency, amongst others. In recent years, due to the overcrowding of the RF spectrum, research interests have shifted towards higher carrier frequencies with major focus on millimetre (mmW) technology for the fifth generation and beyond wireless networks. Note that, all hybrid systems fall into three main fundamental categories in terms of the link loads: (*i*) parallel transmission, where both links are transmitting the same data at the same rate; (*ii*) a dominant link transmission, where the faster and slower links are selected as the default and backup, respectively, and the communications system has to adopt the speed based on the active link; and (*iii*) dual transmission links with different data loads depending on the channel conditions [10].

There are several key applications where the motivation to use a hybrid antenna for both indoor and outdoor applications is clear. For indoor scenarios, femtocell wireless access is attractive, while for outdoor applications front/backhauling is also of an interest [11]. One outdoor application that takes advantage of both VLC and mmW technologies is the vehicular communications. In such networks, the VLC transmitters (Txs) can easily be integrated into vehicle's light-emitting diodes (LEDs)-based head- and tail-lights [12] while the highly directional and high frequency mmW link can result in much reduced inter-channel interference.

To the best of authors' knowledge, no feasible solution has been proposed so far which integrates a hybrid front-end antenna including VLC (with illumination) and mmW in a single package. In addition, the antenna should comply with the three possible hybrid transmission configurations outlined above. Therefore, in this work, we design and experimentally demonstrate a hybrid VLC/planar mmW antenna for an application in vehicular communications networks. The proposed antenna can be used within vehicle's head/tail-lights to provide illumination and data communications simultaneously. The developed VLC transceiver consists of 6 high power white LEDs and two photodiodes (PDs). The planar mmW antenna operates at 20.8 GHz using linear polarisation. Note that, the proposed design procedure is easily transferable to mmW frequencies above 30 GHz so as general we refer it as the mmW design, which can be used in future mmW-based systems. We have adopted quadrature amplitude modulation (QAM) and on-off keying (OOK) for the mmW and VLC links, respectively. This results in less complex modulation and coding schemes but on the other hand reduces the overall system cost-effectiveness and power efficiency. We demonstrate that, links up to 50 Mbaud and 5 Mbps can be realized for the hybrid mmW and VLC links, respectively.

The rest of the paper is organized as follows; Section II with subsections on mmW and VLC describe the structure of the hybrid antenna. Section III discusses the hybrid antenna fabrication, design and the system deployment alongside experimental measurements and performance evaluation. The conclusion is drawn in Section IV.

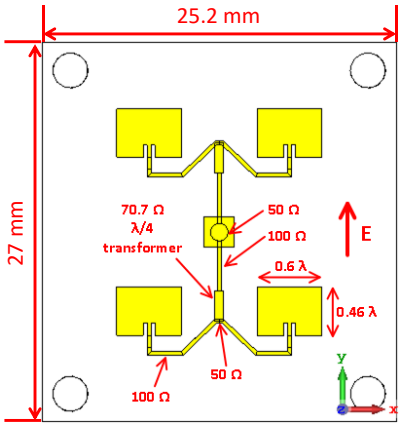

(a)

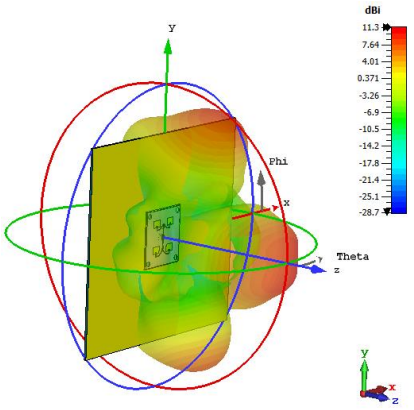

(b)

Fig. 1: (a) Patch antenna diagram showing the dimensions and electric field polarisation. (b) 3D electromagnetic model of the antenna embedded into the board represented by metal and its radiation pattern.

II. Hybrid Antenna Structure

A. The mmW component

The mmW antenna was designed using the CST Microwave Studio [13]. It consists of a four-element microstrip array printed on a 0.5 mm thick Rogers RO4350B substrate with a 25×27 mm^2 antenna printed circuit board (PCB). Note, there is no particular rule for the number of elements in the array antenna. Here, we have adopted a four-element array because of size consideration. The basic radiating element is an inset-fed microstrip antenna with an input impedance of 100 Ω. Note, more on the design of inset-fed can be found in [14, 15]. The two antennas are connected in parallel, yielding 50 Ω, which is transformed via a $\lambda/4$ transformer with an impedance $Z_{\text{tr}} = \sqrt{100 \times 50} = 70.7\ \Omega$ back to 100 Ω. The same is done for the second pair of antennas, resulting in 2×100 Ω in parallel at the centre feeding point, see Fig. 1(a). A detailed schematic of the coupling network is presented in Appendix A. Fig. 1(b) shows the 3D electromagnetic model of the antenna embedded into the board represented by the metal and

This article has been accepted for publication in a future issue of this journal, but has not been fully edited. Content may change prior to final publication. Citation information: DOI 10.1109/ACCESS.2020.3006992, IEEE Access

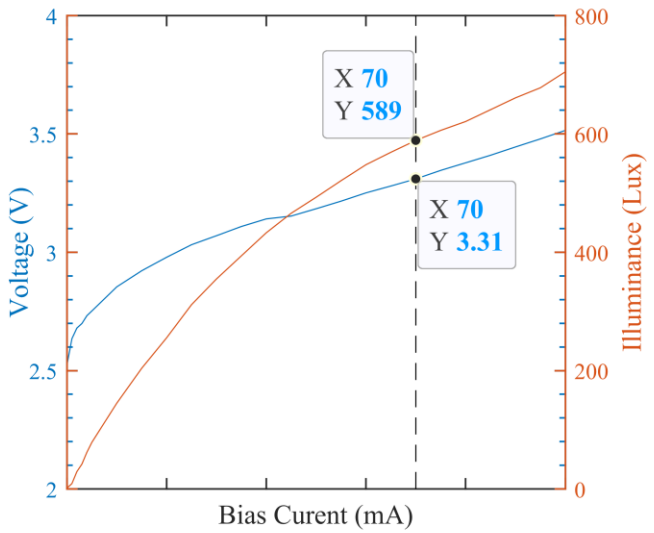

Fig. 3: VI and LI plots of the used LED. The selected LED's bias points are marked on the plots.

its radiation pattern. This figure gives the reader a better idea about how the radiation pattern will look like in manufactured products. The operating frequency is 20.8 GHz with respect to the manufacturing tolerances. A similar approach with different (smaller) connectors and substrate could be adopted and optimised for higher frequency bands if desirable.

B. The VLC component

The VLC Tx circuit is based on a transistor switch circuit with two pairs of three LEDs. A buffer is used to match the data source and the Tx's input impedances. The used white LEDs (Cree C503C-WAN-CCADB231) have a bandwidth of 1.69 MHz. The measured voltage-current (VI) and illuminance-current (LI) characteristics of the LEDs are depicted in Fig. 2. The values of base and emitter resistors are selected to ensure that the transistor is switched between the off and saturated states based on the input signal. The saturation current of the LED is set to 70 mA. Decoupling capacitors are used to isolate both the Tx and the receiver (Rx) from the supply lines to reduces the crosstalk. The optical Rx is composed of a standard PD (Centronics OSD15-5T) and a transimpedance amplifier (TIA, Analog Devices AD8015ARZ). The generated photocurrent is converted into an amplified differential voltage signal prior to low-pass filtering (~10 MHz cut-off frequency) for limiting the out-of-band noise. All VLC circuits were manufactured on FR4. The circuit diagrams as well as details of used components are presented in Appendix A. More information and design guidelines for VLC transceivers are available in [16-20].

The key parameters for both the mmW and VLC components are highlighted in Table I. The VLC section was first simulated using Analog Devices LTspice XVII [21] to verify the circuit functionality and the PCB was designed by

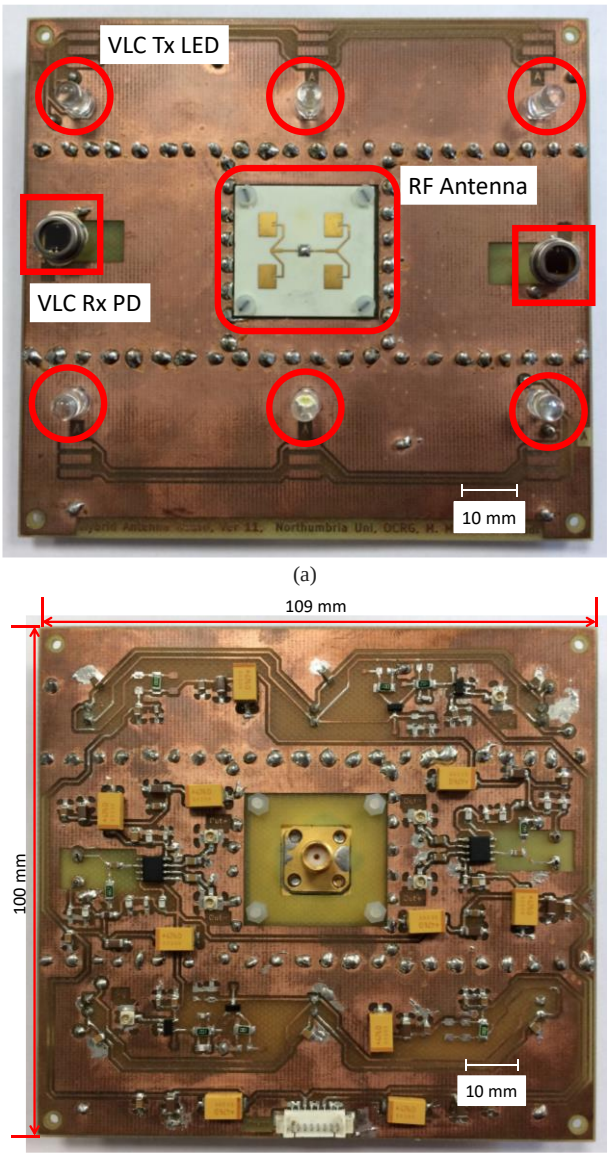

Fig. 2: Fabricated hybrid VLC/mmW antenna: (a) front side and (b) back side. Circle and rectangle show LEDs and PDs, respectively.

KiCAD EDA package version 5 [22]. A photograph of the integrated hybrid antenna is shown in Fig. 3 with the key components highlighted as well as antenna size.

III. Results and Discussion

A. Measurement of the mmW antenna

The normalised simulated and measured radiation patterns and the matching of the mmW antenna are shown in Fig. 4, where a very close agreement can be observed. Note that, the side-lobes in the E-plane have a higher magnitude than those in the H-plane, which is attributed to the surface waves in the substrate. However, the side-lobes can be reduced by various means, e.g., (*i*) decreasing the thickness of the substrate; (*ii*) reducing the relative permittivity of the

This article has been accepted for publication in a future issue of this journal, but has not been fully edited. Content may change prior to final publication. Citation information: DOI 10.1109/ACCESS.2020.3006992, IEEE Access

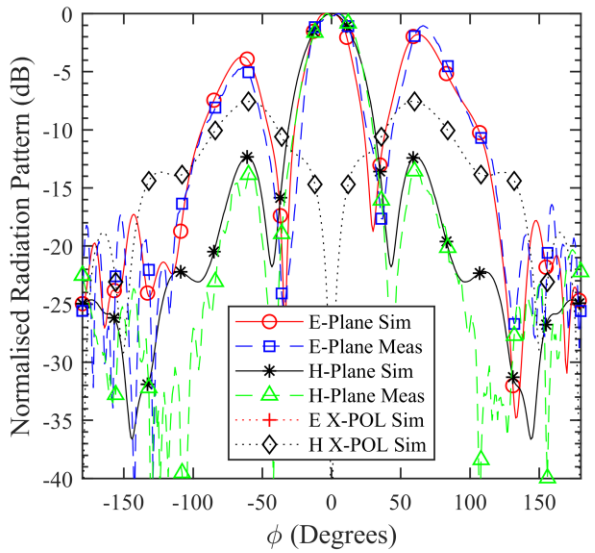

(a)

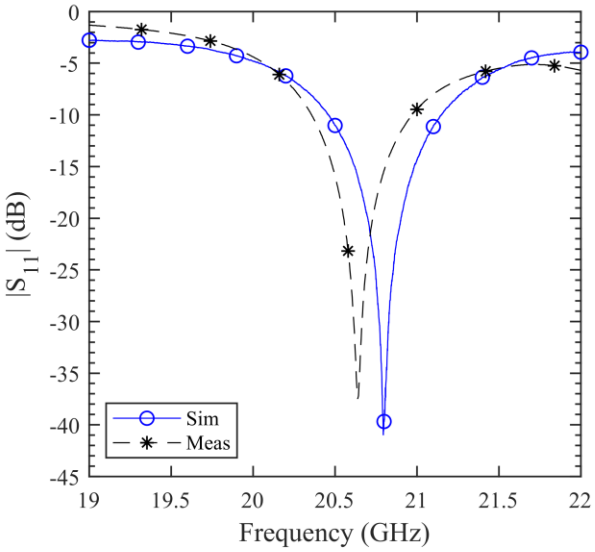

(b)

Fig. 4: Simulation and measurements for the mmW part (Section III.A: Measurement of the mmW antenna): (a) the radiation pattern for E and H planes. Cross polarization in the E-plane is < -80 dB and is not visible in the graph; and (b) the matching (simulated and measured) for the fabricated hybrid antenna.

substrate; or (*iii*) adding a metallic rim around the antenna [23, 24]. However, the downside will be the mechanical stability, the fabrication cost and complexity of the antenna. Note that, for the main lobe the simulated and measured gains are 11.8 and 10.5 dBi, respectively at the 20.8 GHz operating frequency. Note that, the simulated cross polarization result shows a low level (i.e., < -40 dB) along broadside direction.

As shown in Fig. 4(b), the measured centre operating frequency is 20.8 GHz with a relative -10 dB bandwidth of 3.3% (note, the simulated bandwidth is 3%). The marginal differences are attributed to the manufacturing tolerances of the components used and the fact that the catalogue value was used for the substrate permittivity in simulations. Finally, the simulation model depicted in Fig. 1(b) shows the embedded microstrip antenna in a simplified model of the overall hybrid board. Clearly, the metal surface of the VLC board has a negligible impact on the antenna array and its performance.

Table I: Fabricated hybrid antenna parameters

Part	Parameter	Value
VLC	Base resistor	1.41 kΩ
	Emitter resistor	70 Ω
	Decoupling capacitor	220 pF
	Switching transistor	On Semi BSR14
	Photodiode	Centronic OSD15-5T
	LED	Cree 4V white LED
	TIA	Analog Devices AD8015ARZ
mmW	PCB size	25 × 27 mm
	PCB type	0.5 mm thick Rogers RO4350B
	Patch size	4.60 × 3.45 mm^2

To properly evaluate the fabricated hybrid antenna in a real communications system, we carried out two sets of measurements. The 1st and 2nd set of measurements were focused on the performance (i.e., bandwidth and crosstalk) of the mmW and VLC links in parallel, in a laboratory-controlled environment mimicking an outdoor vehicle-to-vehicle communication, respectively. The 802.11p defined channel does not apply here since the standard defines channels at 5.9 GHz due to the short transmission link length of 2 m, which is a typical distance between vehicles in urban areas. In such cases, the line-of-sight is considered to be the dominant transmission path for both VLC and mmW links.

B. VLC link

Here, we have used two hybrid antennas spaced apart by 50 cm and measured the *Q*-factor of the received signal at one antenna at a data rate of 10 Mbps under a dark environment. The measured *Q*-factor as a function of the data rate for a single and multiple LEDs is depicted in Fig. 5(a) along with the horizontal lines equivalent to the *Q*-factor for the BER values of 3.8×10^{-3} (i.e., the forward error correction BER limit) and 10^{-6}. Due to the short distance (i.e., 105 mm) between the LEDs mounted on the PCB, the maximum phase difference between the received signals from any LEDs at a data rate of 10 Mbps is $\sim 1.3^{\circ}$, which is small and thus can be neglected. As shown in Fig. 5(a), the maximum relative difference between the *Q*-factor of one LED and multiple LEDs is 30%. In another test, we carried out an experiment for the link where the VLC Tx of one antenna was fed by a random OOK signal while the Rx was receiving a signal from a separate light source. We carried

This article has been accepted for publication in a future issue of this journal, but has not been fully edited. Content may change prior to final publication. Citation information: DOI 10.1109/ACCESS.2020.3006992, IEEE Access

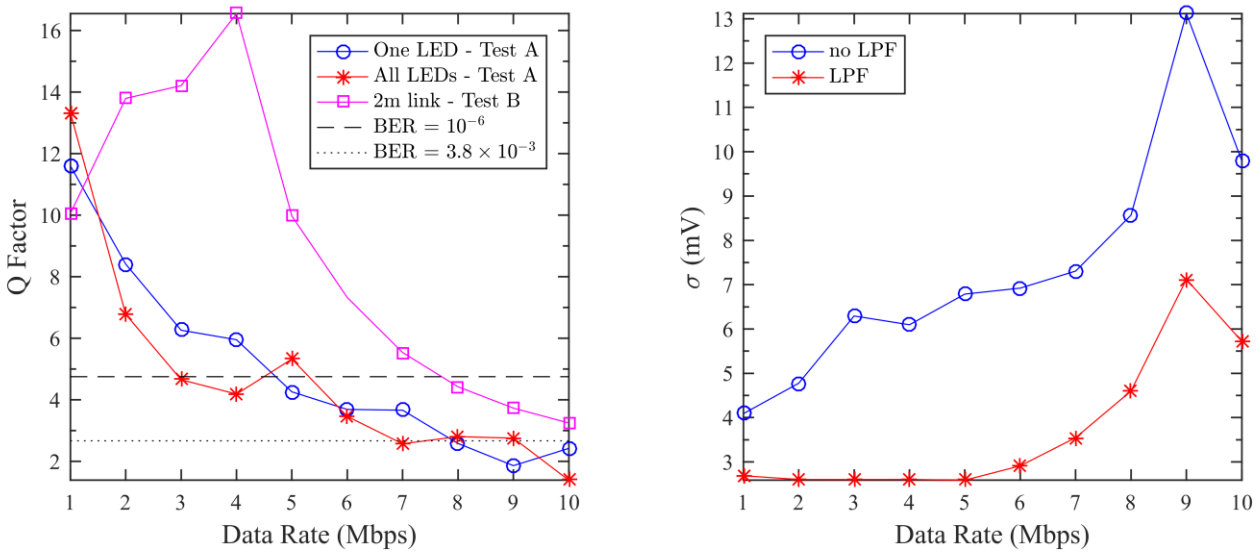

(a) (b)

Fig. 5: (a) The Q-factor as a function of the data rate for the hybrid antenna with a single LED and all LEDs (Section III.B: VLC test) and for the BER values of 3.8×10^{-3} and 10^{-6}. Also shown is the performance of VLC Tx over a 2 m link (Section III.C: hybrid VLC/MMW antenna implementation in a real system). (b) Standard deviation versus the data rate for theRx output voltage before and after LPF (Section III.B: VLC test).

out the measurement with and without the low pass filter (LPF) for the data rate in the range of 1 to 10 Mbps, see Fig. 5(b). What we observed was that, for the case with no LPF, the sudden switch toggle of the Tx resulted in power line voltage drop. On the other hand, the Rx circuit with a feedbacked amplifier stage (e.g., the TIA section) is affected by this supply voltage drop, thus resulting in a damped ringing signal with the frequency of 78.8 MHz embedded in the output of TIA. This unwanted signal coupling can be removed by fabricating the circuit on multilayers PCBs with dedicated power planes, decoupling capacitors on the power lines and power pins of the components. However, since the ringing frequency is out of the VLC/mmW signal frequency range, we simply used an LPF at the output of the TIA. Note that, using the via stitching technique on the PCB we have increased the isolation between the Tx and the Rx sections.

B. Hybrid VLC/mmW antenna implementation in a real system

Finally, we carried out measurements for both links being active over a 2 m long transmission link using the block diagram illustrated in Fig. 6. The VLC Tx was fed with a 10^5 bit long pseudorandom binary sequence (PRBS) signal using a waveform generator (Teledyne T3AWG3252). In order to properly quantify the Tx performance, the VLC Rx included a Fresnel lens (diameter and focal length of 63 mm and 6.6 mm, respectively) and an optical Rx (Thorlabs APD430A2/M). The electrical signal was captured using a

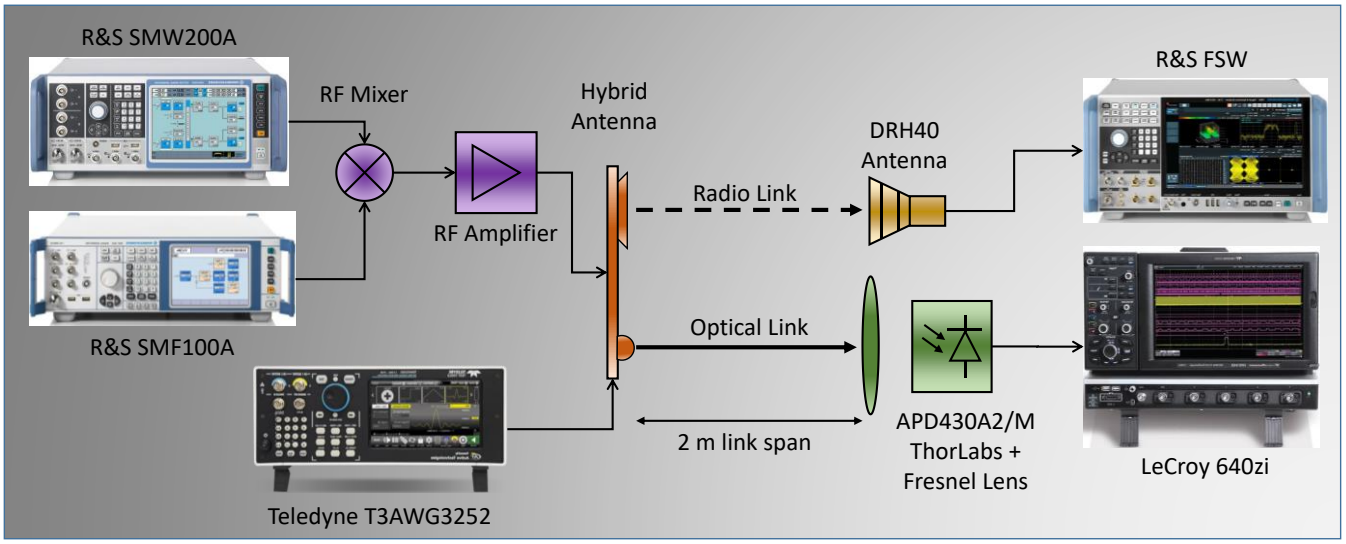

Fig. 6: A block diagram of the experimental setup for the hybrid VLC/mmW antenna under the real system test environment.

This article has been accepted for publication in a future issue of this journal, but has not been fully edited. Content may change prior to final publication. Citation information: DOI 10.1109/ACCESS.2020.3006992, IEEE Access

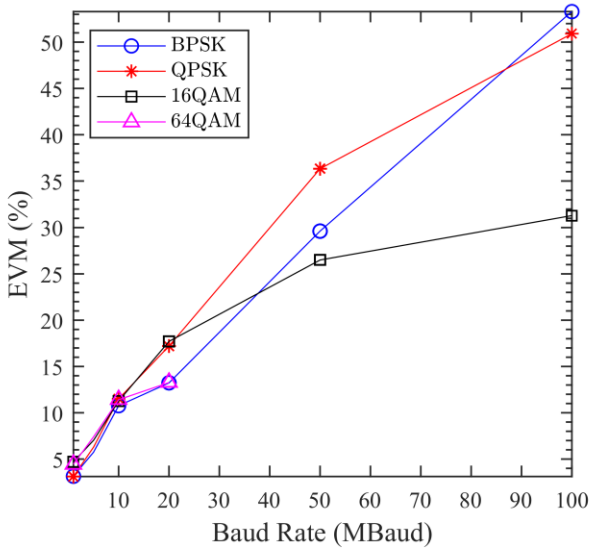

Fig. 7: Measured EVM of mmW link over 2 m experimental setup for different digital mmodulation schemes link (Section III.C: hybrid VLC/mmW antenna implementation in a real system).

real-time sampling storage scope (LeCroy Waverunner 640Zi) for further offline processing. Here, we also measured the *Q*-factor of the received signal for a range of data rates, see the purple curve in Fig. 5(a). For the 2 m case, we notice an unexpected peak in the plot, which is simply caused by frequency response of the optical Rx. The optical Rx has a low cut-off frequency acting as a high pass filter, thus the increase of the Q-factor for frequencies below 4 MHz. However, as frequency increases the LED frequency response become the dominant factor, which leads to deterioration of the circuit performance. The peak at around 3 to 4 MHz is expected, which coincide with the frequency range of the white LED.

As for the mmW section, the antenna was fed by a 20.8 GHz RF signal. Here, binary phase shift keying (BPSK), quadrature phase shift keying (QPSK), 16- and 64-QAM at the symbol rates in the range of 1 to 100 Mbaud were used. The signals

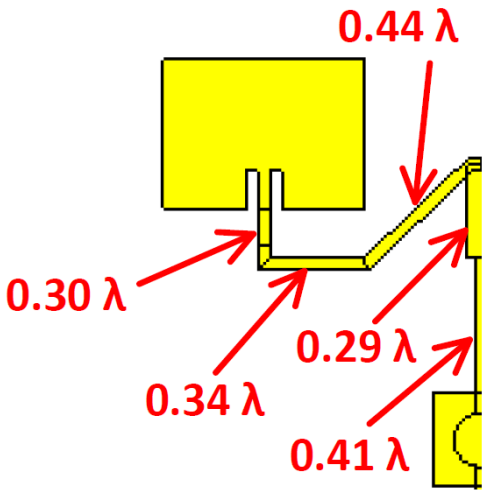

Fig A.1: Detailed diagram of the coupling network of RF antenna.

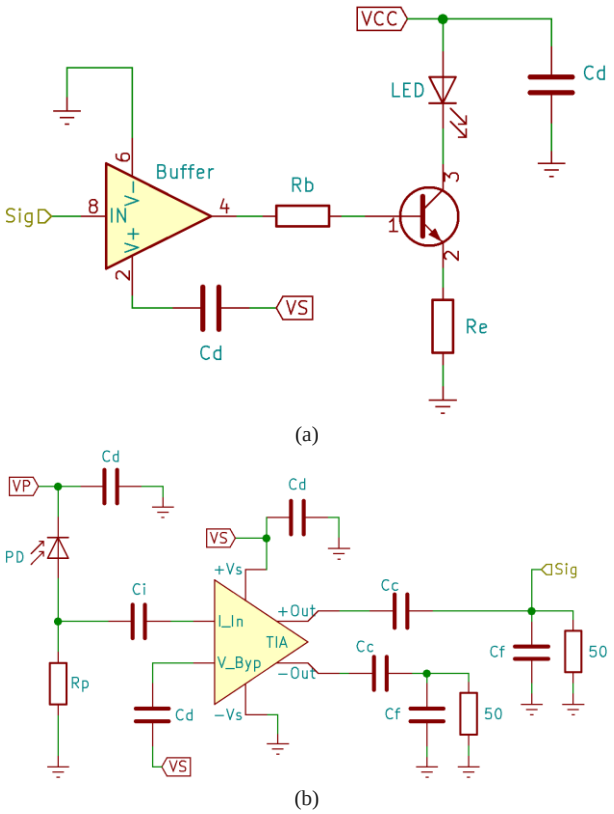

Fig. A.2: a) Tx switching circuit blockdiagram, and b) Rx transimpedance amplifier (TIA) circuit blockdiagram.

were generated using a signal generator (R&S SMW200A), and then up-converted to the desired frequency using a mixer and carrier generator (R&S SMF100A) followed by amplification using a low-noise RF amplifier (Analog Devices HMC1131). Similar to the VLC section, to appropriately qualify the antenna performance, a double ridged horn antenna (DRH40 – RFspin, s.r.o.) with a gain of 14 dBi at 20.8 GHz was used at the Rx. The evaluation of the received signal in terms of the received electrical power and the error vector magnitude (EVM) using a signal analyser (R&S FSW) is illustrated in Fig. 7. As can be observed, with no equalisation and using multi-level modulation techniques, the hybrid antenna offers the minimum data rates of 5 Mbps and 50 Mbaud for VLC and mmW, respectively, which is sufficient for low-data rates applications such as vehicular communications. Moreover, our investigation demonstrated the operation of the proposed hybrid antenna for the following cases: (*i*) parallel transmission of VLC and mmW at a data rate of 5 Mbps; (*ii*) mmW and VLC serving as the default and backup links with data rates of 50 Mbaud and 5 Mbps, respectively; and (*iii*) mmW and VLC operating depending on the channel conditions, where for a clear channel the data rate could exceed 50 Mbaud.

IV. Conclusion

We proposed a hybrid VLC/mmW antenna featuring illumination, and data transmission for use in vehicular

Table A.I: Fabricated VLC transceiver parameters

Parameter	Value
R_b	1.41 kΩ
R_e	70 Ω
R_p	7 kΩ
C_d	220 pF
C_i	10 nF
C_c	47 µF
Buffer	NC7SZ08M5X
Transistor	BSR14
Photodiode	OSD15-5T
LED	Cree 4V white LED
TIA	AD8015ARZ
VS	+5 V
VP	+12 V

communications. The paper outlined the new design of mmW antenna and the supporting Tx and Rx circuits for VLC. First, we assessed the characteristics of VLC and mmW sections individually and then evaluated the performance of the proposed antenna in a mimicked real scenario by measuring the *Q*-factor and the EVM for VLC and mmW links, respectively. The results showed that, the minimum data rates of 5 Mbps and 50 Mbaud for VLC and mmW, respectively are perfectly achievable. Our measurement showed that, a BER of 10^{-6} and an acceptable EVM value for VLC and mmW links for each modulation scheme, respectively. Therefore, we showed that the proposed hybrid antenna can provide reliable VLC and mmW links (i.e., illumination and data transmission) in future vehicular communications.

APPENDIX A

RF Antenna

The detailed dimensions of the coupling network from Fig. 1(a) is presented in Fig. A.1.

VLC Transceiver

Fig. A.2 shows the circuit diagram of the VLC Tx and Rx while Table A.I summarises the used components values.

REFERENCES

[1] B. Bag, A. Das, I. S. Ansari, A. Prokeš, C. Bose, and A. Chandra, "Performance analysis of hybrid FSO systems using FSO/RF-FSO link adaptation," *IEEE Photonics Journal*, vol. 10, no. 3, pp. 1-17, 2018.

[2] S. Enayati and H. Saeedi, "Deployment of Hybrid FSO/RF Links in Backhaul of Relay-Based Rural Area Cellular Networks: Advantages and Performance Analysis," *IEEE Communications Letters*, vol. 20, no. 9, pp. 1824-1827, 2016.

[3] J. Kong, M. Ismail, E. Serpedin, and K. A. Qaraqe, "Energy Efficient Optimization of Base Station Intensities for Hybrid RF/VLC Networks," *IEEE Transactions on Wireless Communications*, vol. 18, no. 8, pp. 4171-4183, 2019.

[4] D. A. Basnayaka and H. Haas, "Hybrid RF and VLC Systems: Improving User Data Rate Performance of VLC Systems," in *2015 IEEE 81st Vehicular Technology Conference (VTC Spring)*, 2015, pp. 1-5.

[5] K. O. Odeyemi and P. A. Owolawi, "Selection combining hybrid FSO/RF systems over generalized induced-fading channels," *Optics Communications*, vol. 433, pp. 159-167, 2019/02/15/ 2019.

[6] F. Nadeem, B. Geiger, E. Leitgeb, S. S. Muhammad, M. Loeschnig, and G. Kandus, "Comparison of link selection algorithms for free space optics/radio frequency hybrid network," *Communications, IET*, vol. 5, no. 18, pp. 2751-2759, 2011.

[7] A. Arockia Bazil Raj, J. Arputha Vijaya Selvi, and S. Durairaj, "Comparison of different models for ground-level atmospheric turbulence strength (Cn2) prediction with a new model according to local weather data for FSO applications," *Applied Optics*, vol. 54, no. 4, pp. 802-815, 2015/02/01 2015.

[8] J. Tóth, Ľ. Ovseník, J. Turán, L. Michaeli, and M. Márton, "Classification prediction analysis of RSSI parameter in hard switching process for FSO/RF systems," *Measurement*, vol. 116, pp. 602-610, 2018/02/01/ 2018.

[9] M. Najla, P. Mach, Z. Becvar, P. Chvojka, and S. Zvanovec, "Efficient Exploitation of Radio Frequency and Visible Light Communication Bands for D2D in Mobile Networks," *IEEE Access*, vol. 7, pp. 168922-168933, 2019.

[10] M. M. Abadi, Z. Ghassemlooy, S. Zvanovec, M. R. Bhatnagar, and Y. Wu, "Hard switching in hybrid FSO/RF link: Investigating data rate and link availability," in *2017 IEEE International Conference on Communications Workshops (ICC Workshops)*, 2017, pp. 463-468.

[11] M. B. Rahaim and T. D. C. Little, "Toward practical integration of dual-use VLC within 5G networks," *IEEE Wireless Communications*, vol. 22, no. 4, pp. 97-103, 2015.

[12] B. Turan, O. Narmanlioglu, S. C. Ergen, and M. Uysal, "Physical layer implementation of standard compliant vehicular VLC," in *2016 IEEE 84th Vehicular Technology Conference (VTC-Fall)*, 2016, pp. 1-5: IEEE.

[13] (21/11/2019). *CST Microwave Studio*. Available: https://www.3ds.com/products-services/simulia/products/cst-studio-suite/electromagnetic-systems/

[14] P. Sharma, S. K. Koul, and S. Chandra, "Micromachined inset-fed patch antenna at Ka-band," in *2006 Asia-Pacific Microwave Conference*, 2006, pp. 693-696.

[15] H. Ying, D. R. Jackson, J. T. Williams, and S. A. Long, "A design approach for inset-fed rectangular microstrip antennas," in *2006 IEEE Antennas and Propagation Society International Symposium*, 2006, pp. 1491-1494.

[16] K. Modepalli and L. Parsa, "Lighting Up with a Dual-Purpose Driver: A Viable Option for a Light-Emitting Diode Driver for Visible Light Communication," *IEEE Industry Applications Magazine*, vol. 23, no. 2, pp. 51-61, 2017.

[17] K. Modepalli and L. Parsa, "Dual-Purpose Offline LED Driver for Illumination and Visible Light Communication," *IEEE Transactions on Industry Applications*, vol. 51, no. 1, pp. 406-419, 2015.

[18] T. Kishi, H. Tanaka, Y. Umeda, and O. Takyu, "A High-Speed LED Driver That Sweeps Out the Remaining Carriers for Visible Light Communications," *Journal of Lightwave Technology*, vol. 32, no. 2, pp. 239-249, 2014.

[19] P. Horowitz and W. Hill, *The art of electronics*. Cambridge Univ. Press, 1989.

[20] F. Che, L. Wu, B. Hussain, X. Li, and C. P. Yue, "A Fully Integrated IEEE 802.15.7 Visible Light Communication Transmitter With On-Chip 8-W 85% Efficiency Boost LED Driver," *Journal of Lightwave Technology*, vol. 34, no. 10, pp. 2419-2430, 2016/05/15 2016.

[21] (12/11/2019). *LTspice*. Available: https://www.analog.com/en/design-center/design-tools-and-calculators/ltspice-simulator.html

[22] (12/11/2019). *KiCad EDA*. Available: http://www.kicad-pcb.org/

[23] D. M. Pozar, *Microwave engineering*, 2nd ed. ed. New York ,Chichester: Wiley, 1998.

[24] M. T. Nguyen, B. Kim, H. Choo, and I. Park, "Effects of a cavity structure on a half E-shaped microstrip patch antenna," in *2011 International Workshop on Antenna Technology (iWAT)*, 2011, pp. 310-313.